Erroneous fold tests as an artifact of alteration chemical remanent magnetization

Karen Nørgaard Madsen and Harald Walderhaug
University of Bergen, Institute of Solid Earth Physics, Bergen, Norway

Trond Torsvik
VISTA, Geological Survey of Norway, Trondheim, Norway

Received 19 June 2001; revised 31 March 2002; accepted 4 April 2002; published 26 December 2002.

[1] Several studies have shown that an alteration chemical remanent magnetization (CRM) may have a direction intermediate between that of the remanence of the parent phase and the field during remagnetization. In a fold a surviving natural remanent magnetization (NRM) is exposed at varying angles to the remagnetizing field, giving rise to varying degree of remanence deflection. A laboratory experiment was carried out to investigate how the CRM deflection varies with angle between parent phase NRM and remagnetizing field, H_{CRM}, and we discuss how this variation would affect the results of a fold test. The experiment was performed on a Silurian lava, with a well-defined single component NRM carried by deuterically oxidized titanomagnetite (TM). Specimens of the lava were arranged in a fold configuration with NRM at various angles to a 50 μT laboratory field. Heating to 525°C resulted in oxidation of part of the primary TM phase to hematite, leading to the formation of stable remanence components of intermediate direction, as revealed by thermal demagnetization. Stepwise unfolding of the CRM gave a syntectonic fold test result. The variation of remanence deflection with angle between H_{CRM} and initial NRM can be understood in terms of vector addition of fields or remanence components. A model for CRM acquisition derived from the experimental results was employed to explore CRM in other fold configurations. It appears from analysis of synthetic data that it is possible to falsely conclude both synfold and prefold magnetization from fold tests on postfold or synfold CRM. *INDEX TERMS:* 1525 Geomagnetism and Paleomagnetism: Paleomagnetism applied to tectonics (regional, global); 1533 Geomagnetism and Paleomagnetism: Remagnetization; 1540 Geomagnetism and Paleomagnetism: Rock and mineral magnetism; 1594 Geomagnetism and Paleomagnetism: Instruments and techniques; *KEYWORDS:* paleomagnetism, rock magnetism, remagnetization, CRM, alteration CRM, fold tests

Citation: Madsen, K. N., H. Walderhaug, and T. Torsvik, Erroneous fold tests as an artifact of alteration chemical remanent magnetization, *J. Geophys. Res.*, *107*(B12), 2369, doi:10.1029/2001JB000805, 2002.

1. Introduction

[2] Alteration chemical remanent magnetization (CRM) is formed by the transformation of one magnetic mineral into another under the influence of an external field. In cases where a change of crystal lattice is involved, several investigations have revealed stable CRM components with directions intermediate between the preexisting remanence and the remagnetizing field [*Bailey and Hale*, 1981; *Heider and Dunlop*, 1987; *Walderhaug et al.*, 1991; *Walderhaug*, 1992].

[3] *Heider and Dunlop* [1987] studied alteration CRM using specimens of synthetic magnetite which were given an ARM as the parent phase remanence. The oxidation product was a mixture of a cation deficient spinel phase and hematite, and the CRM resulting from the alteration had directions intermediate between the ARM and the field during oxidation, H_{CRM}. On the basis of their results with varying strength of ARM and H_{CRM}, Heider and Dunlop proposed that CRM formed parallel to a resulting field being the sum of H_{CRM} and a field proportional to the parent phase magnetization (ARM):

$$\mathbf{CRM} \parallel (\mathbf{H}_{CRM} + \beta \cdot \mathbf{ARM}). \quad (1)$$

When this model is valid for natural rocks, with NRM replacing ARM as the parent phase magnetization, the deflection of CRM from parent phase natural remanent magnetization (NRM) depends on the angle between NRM and H_{CRM}. Because of this angular dependence the degree of remanence deflection by alteration CRM formation will vary over a fold where a surviving NRM is exposed at various angles to the remagnetizing field. A systematic variation of deflections could likely affect the results of fold tests. This paper reports the results of a CRM experiment carried out on natural rock to test the validity of equation (1)

0148-0227/02/2001JB000805$09.00

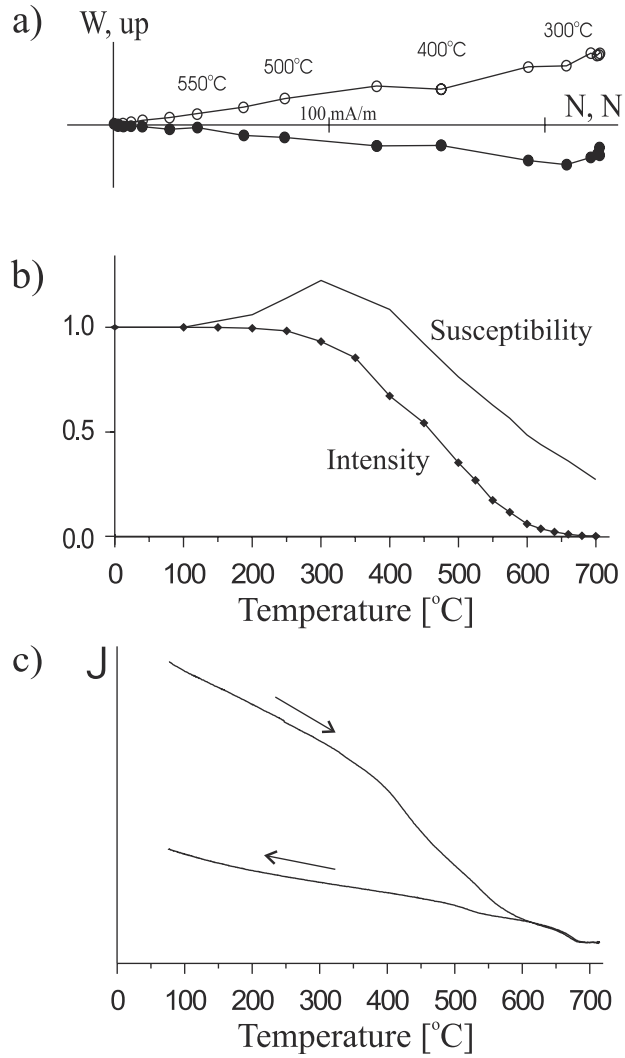

Figure 1. (a) Zijderfeld diagram obtained from thermal demagnetization of pilot specimen NRM. Solid/open circles in the orthogonal plot represent points in the horizontal/vertical plane. (b) Relative intensity and susceptibility of the same specimen as functions of demagnetization temperature. (c) Thermomagnetic analysis of untreated material, curve obtained in a field of 800 mT.

with varying angle between remagnetizing field and parent phase NRM, and discuss its implications for fold tests.

2. Starting Material

[4] The rock used for the experiment was a Silurian lava flow from Crawton Bay on the Scottish coast, south of Aberdeen (56°54′N, 2°12′W). From previous CRM experiments on this rock [*Walderhaug et al.*, 1991; *Walderhaug*, 1992] it was known to possess the desired qualities for this study; a stable univectorial NRM, negligible anisotropy of susceptibility (AMS) and a relatively uniform magnetic mineralogy. Finally it had proven predisposed for chemical alteration of a magnetic phase resulting in stable CRM components of intermediate direction.

[5] Twenty-five cylindrical specimens were retrieved from one hand sample of the lava. Two of the specimens had spurious NRM magnetizations and were discarded, while the rest show a tight grouping (*Fisher* [1953] precision parameter $k = 1992$) of NRM directions with mean $D = 1.1$, $I = -7.2$ in sample coordinates. No significant change of magnetization direction was encountered during thermal and alternating field (AF) demagnetization of three and two pilot specimens, respectively, so the NRM is confirmed to be essentially a single component magnetization (Figure 1a). NRM intensities of the 23 specimens range from 206 to 363 mA/m with an average of 282 mA/m. Susceptibilities range from 1068 to 3024 (10^{-6} SI) with an average of 2488 (10^{-6} SI). AMS was determined before and after the experiment and revealed very little anisotropy (measured oblate and prolate deviations from perfect isotropy less than 0.4%).

[6] A large fraction of the NRM intensity resides in grains of high coercivity. AF demagnetization to 250 mT left the two pilot specimens with more than 40% of the NRM intensity intact. Thermal demagnetization of a 3-component isothermal remanent magnetization (IRM) following the procedure of *Lowrie* [1990], showed that the large remanence component associated with coercivities in excess of 300 mT survived to 680°C, indicating that it is carried by hematite.

[7] The presence of hematite is also obvious from thermomagnetic analysis (Figure 1c) showing Curie temperatures of 670–680°C. Another Curie point close to that of magnetite is inferred at temperatures between 545°C and 580°C for the heating curves and somewhat lower, at around 540°C, for the cooling curves. Finally, the heating curves often have an inflection point around 400°C attesting to some low temperature oxidation. The Curie curves are irreversible and only part of the intensity is recovered after heating due to transformation of the spinel phase to hematite. If the more cation deficient part of the spinel phase is more vulnerable to this transformation, then this may explain the lowering of the ''near magnetite'' Curie point. Reflected light microscopy revealed deuterically oxidized grains of titanomagnetite with exsolved ilmenite lamellae. The Curie temperatures close to T_C of magnetite are probably associated with the titanium poor phase between the lamellae, and suggest that this phase is close to magnetite composition. Hysteresis properties were measured in a peak field of 1T. For untreated material H_c, as determined from three samples, varied from 14.5 to 19.2 mT and J_{rs}/J_s varied from 0.19 to 0.23, indicating grains in the pseudosingle-domain range.

3. Experimental Procedure

[8] Specimens were arranged with NRM at angles 25°, 45°, 60°, 75°, 90°, 105°, 120°, 135° and 155° to a laboratory field, H_{CRM}, applied during CRM formation (Figure 2). Hence the experiment simulates a situation where CRM is formed in a folded rock and also provides data useful for

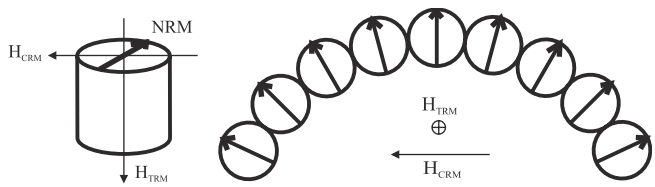

Figure 2. Sketch showing the configuration of samples and fields during the CRM treatment.

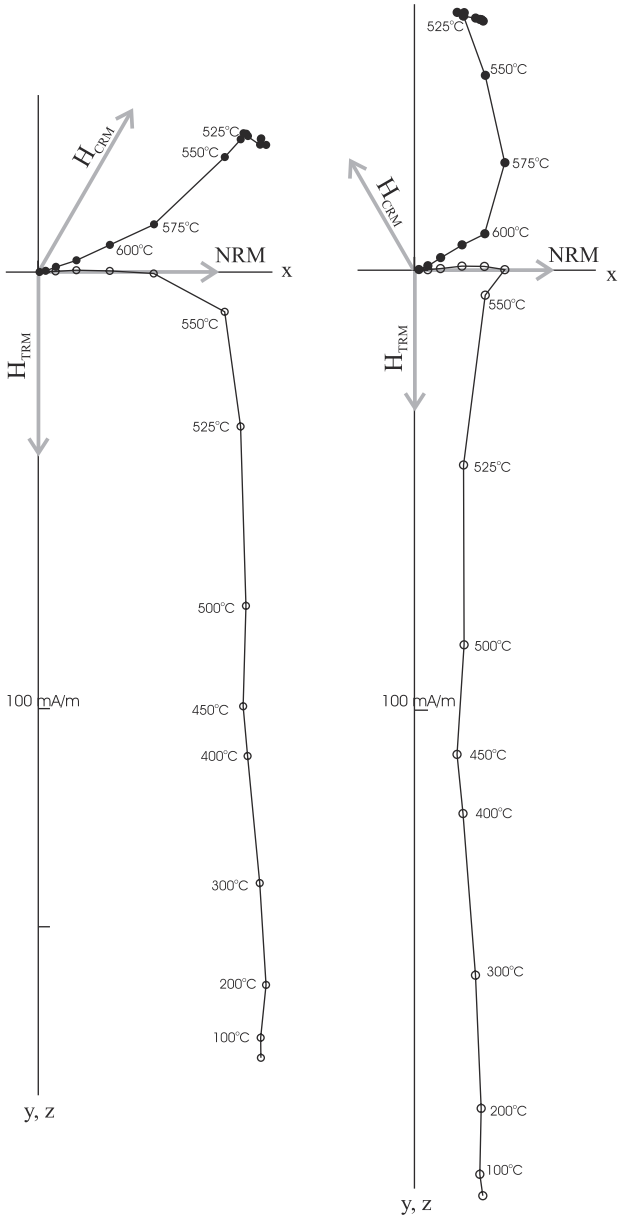

Figure 3. Two examples of Zijderveld diagrams obtained from thermal demagnetization after the CRM treatment. The specimens acquired CRM with initial NRM at angles 60° and 120°, respectively, to H_{CRM}. In the diagram the *x*-*y* plane (solid circles) is the cylinder plane of the specimens. Directions of H_{CRM} and NRM in this plane are indicated by arrows. The *x*-*z* plane (open circles) is spanned approximately by NRM and H_{TRM}, with H_{TRM} parallel to the *z* axis.

investigating the dependence of intermediate CRM direction on angle between parent phase NRM and the field during alteration. H_{CRM} had a strength of 50 μT, and was applied perpendicular to the cylinder-axis (the *z* axis) of the specimens which were arranged on the oven platform with sample x-coordinates (from which the NRM directions were inclined only −6° to −8°) at individual angles to the field. CRM formation took place at a temperature of 525°C, maintained for 5 hours. In laboratory experiments on CRM, specimens are often allowed to cool in zero field to avoid TRM acquisition. This situation would never occur in nature, and it is desirable to assess the influence of a TRM adding to the CRM. As the oven was turned off, the field strength was therefore maintained, but the direction was switched to parallel the *z* axis of the specimens. By this procedure TRM acquired during cooling was directed almost perpendicular to the plane of NRM and H_{CRM} to clearly distinguish it from the CRM.

[9] After this treatment the specimens were thermally demagnetized, using 30 min at peak temperature for each step. To monitor the degree of chemical alteration due to the CRM treatment and the subsequent thermal demagnetization, bulk susceptibility of the specimens was measured at room temperature before and after heating in H_{CRM}, and after each step of thermal demagnetization.

4. Results

[10] In Figure 3, two examples of thermal demagnetization results are presented in Zijderveld diagrams. At temperatures up to about 525°C, the temperature of CRM acquisition, unblocked remanence has a direction (I = 89.5°, D = 80.2°, k = 2221, α_{95} = 0.7) indistinguishable from that of H_{TRM} (Figure 4). As temperatures exceed 525°C the H_{TRM} component is rapidly reduced as expected for a partial thermoremanent magnetization (pTRM) acquired during

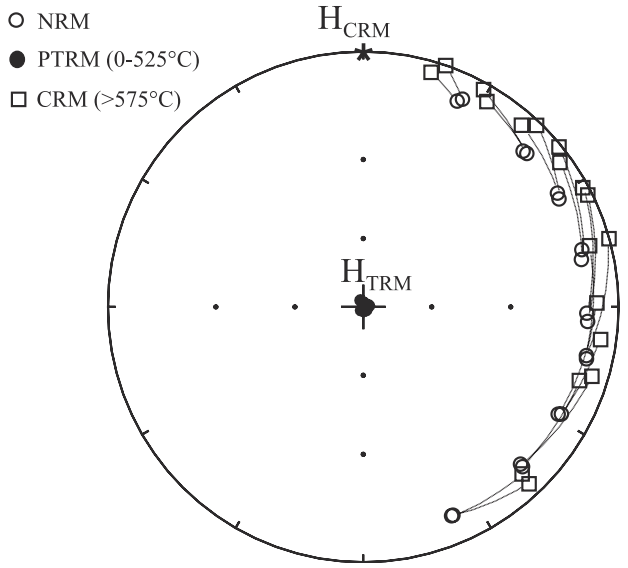

Figure 4. Summary of remanence components of low and high blocking temperature for all specimens, shown in a stereographic projection, with the H_{CRM} direction (star) kept fixed in space. The components isolated for demagnetization temperatures up to 525°C (down-pointing) are extremely tightly grouped and parallel to H_{TRM} (I = 90°, marked by central cross) within experimental error. Open circles denote (up-pointing) initial NRM directions for individual specimens. Open squares denote (up-pointing) stable end components (CRM) removed by demagnetization above 575°C. Great circle trajectories join NRM and CRM points from the same specimens. The CRM components are intermediate between initial NRM and H_{CRM}, except for a small deflection toward H_{TRM}.

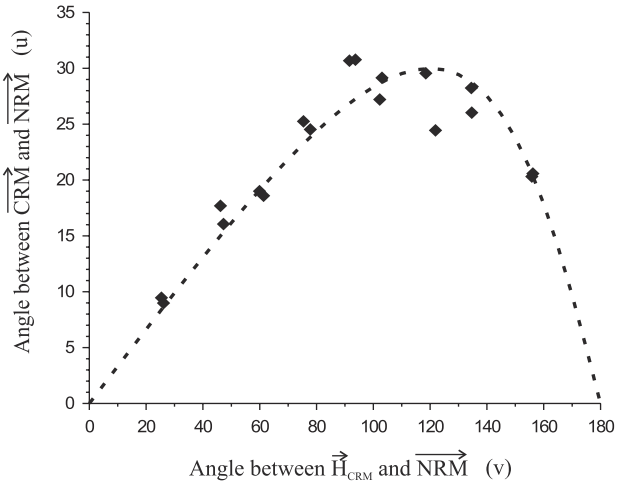

Figure 5. Angle of deflection, u, of the CRM component from the original NRM direction as a function of the angle v between NRM and the laboratory field during CRM acquisition. The dashed curve shows the relationship derived from Figure 6.

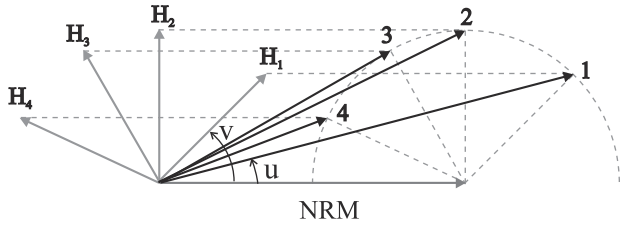

Figure 6. Vectorial addition of components parallel to NRM and H_{CRM} (grey vectors) in proportion 2:1. Four examples are given with H_{CRM} (H_1–H_4) applied at angles v = 45, 90, 120, and 155° to the NRM. The deflection of the resulting vector (CRM) from the NRM direction first increases with v (cases 1–3), and then decreases for the highest angles (case 4). The length of the resulting component decreases with increasing v.

cooling from 525°C to room temperature [*Pullaiah et al.*, 1975; *Walton*, 1980]. Only about 5 and 2% of this component survive demagnetization to 550°C and 575°C, respectively. A small remanence component in the direction of H_{TRM} did however persist throughout the demagnetization, deflecting the inferred CRM directions a few degrees out of the plane spanned by NRM and H_{CRM}. In this plane the first temperature steps above 525°C moves the remanence away from H_{CRM} and toward the initial NRM direction. From 575, 600, or in a few cases 620°C, stable end components with directions between H_{CRM} and the original NRM could be isolated for all specimens. These components, which will tentatively be termed CRM, are shown for all specimens in Figure 4 together with individual NRM directions and the common direction of H_{CRM}. Susceptibility decreased by 45 to 70% during the CRM treatment at 525°C, and another 10–20% during subsequent thermal demagnetization at temperatures in excess of 525°C.

5. Discussion

5.1. CRM Direction

[11] CRM directions are intermediate between H_{CRM} and parent phase NRM, except for a few degrees deflection in the direction of H_{TRM}. In nature the field configuration is unlikely to change dramatically during CRM formation and cooling, and the small contribution from TRM would more likely add in the direction of H_{CRM}. In the following discussion, v denote the angle between H_{CRM} and parent phase NRM and u denote the angle between NRM and the obtained direction of CRM. The presence of the small TRM component changes u on average 0.5° and will be neglected in the discussion. Figure 5 shows u plotted as a function of v. Starting at low values of v, u increases almost linearly with v until the two components are close to perpendicular, then the development slows down and turns to a decrease for high angles.

[12] The ratio of intensity parallel to NRM and parallel to H_{CRM} for the last demagnetization steps is close to 2 for all specimens, and the trend in the data is modeled quite well by simply adding vectorially components along NRM and H_{CRM} in proportion 2:1, as illustrated by Figure 6. This model is equivalent to equation (1) with the component in the direction of NRM assumed constant although NRM intensity does vary between specimens. As will be discussed in section 5.2, the variation is more likely due to varying concentration of the parent phase than varying efficiency of magnetization as in the experiment of *Heider and Dunlop* [1987], which may explain the apparently different results.

5.2. CRM Intensity and Origin of the Remanence

[13] Exploring the dependence of CRM intensity on angle between NRM and H_{CRM} is complicated by a strong correlation of CRM intensity with initial NRM intensity. Figure 7 shows this correlation using the remanence remaining after heating to 600°C, decomposed along the directions of NRM, H_{CRM} and H_{TRM}. The strength of each component

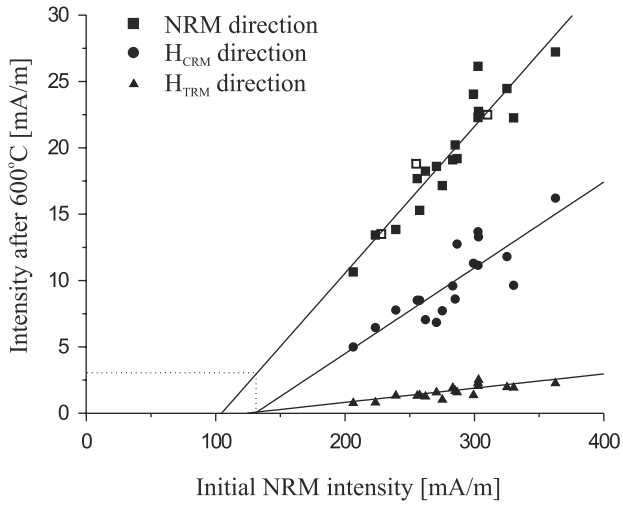

Figure 7. Strength of remanence after thermal demagnetization to 600°C in the direction of NRM (squares), H_{CRM} (circles) and H_{TRM} (triangles) plotted versus initial NRM strength of the specimens. Open symbols indicate NRM remaining at the same temperature step for untreated pilot samples. The lines are best fit to data (linear regression), and intersect the x axis at 105 and 130 mA/m for NRM and H_{CRM} components, respectively.

varies in proportion to the part of initial NRM intensity exceeding a "ground level" of 105 and 130 mA/m for the NRM and H_{CRM} component, respectively. This level probably corresponds to a more or less constant contribution to initial NRM from hematite which is not participating in the CRM formation. AF demagnetization to 250 mT of fresh specimens supports this interpretation, revealing that the removed intensity was strongly correlated to initial intensity, while the remaining hard component was similar in size to the ground level deduced from Figure 7 and uncorrelated with initial intensity.

[14] To eliminate the effect of the variability of initial NRM strength, CRM intensities were normalized by division with initial NRM intensity [mA/m] minus 117 mA/m, which was the value chosen for the ground level (it makes little difference which value between 105 and 130 mA/m is used). After normalization the CRM intensity is seen to decrease with increasing angle between NRM and H_{CRM} (Figure 8) in good agreement with the decrease of the length of the resultant vector (CRM) in Figure 6.

[15] There are two different physical interpretations of the model in Figure 6: (1) The components represent fields, the external field and an internal field proportional to NRM, and CRM forms parallel to the resultant field, and (2) the components represent remanence and CRM is the vector sum of remanence in the directions of NRM and H_{CRM}. According to interpretation 2 the length of the resultant vector in Figure 6 describes directly the strength of the CRM. In interpretation 1 it does not describe the CRM itself, but the strength of the resultant field in which CRM forms. Earlier CRM experiments on the same rock with varying strength of H_{CRM} showed that CRM intensity was proportional to the field strength [*Walderhaug*, 1992]. When this is the case the same conclusion will be drawn as for interpretation 1, and the variation of CRM intensity with v does not offer a possibility to determine whether interpretation 1 or 2 or a mix of both is correct.

[16] Other evidence indicates that surviving NRM in the hematite phase is hardly the main contribution to the NRM component of "CRM." Demagnetization performed on specimens from another hand sample of the same rock demonstrated that the remanence intensity remaining after stepwise demagnetization of NRM up to 600°C was about 3 times higher than after one single heating to 600°C. Since the latter procedure leaves less time for CRM formation to take place during the demagnetization, this result suggests that preexisting hematite components of NRM contributes less than 1/3 to the "NRM intensity" present after stepwise demagnetization of untreated specimens to 600°C. The dominant part must be of CRM origin and is similar in size to the NRM component of CRM for treated specimens (Figure 7). The interpretation of Figure 7 also indicates a small or absent contribution of surviving NRM to the CRM of treated specimens. The x-axis intercepts of the linear interpolation lines predict that for a sample of ground level intensity, i.e., with no CRM forming fraction, roughly all remanence would be removed after demagnetization to 600°C or, if the small difference in intercept of the linear fits for the NRM and the H_{CRM} components is not taken to be a coincidence, that a small surviving NRM of about 3 mA/m remains for a sample of ground level remanence 130 mA/m.

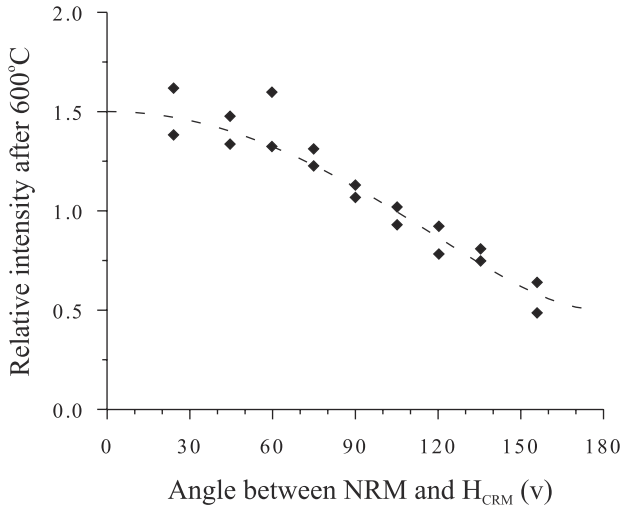

Figure 8. Intensity of remanence (arbitrary scale) remaining after thermal demagnetization to 600°C, normalized to eliminate the effect of varying initial NRM intensity (see text), and plotted versus angle between NRM and H_{CRM}. The dashed curve indicates the decrease as derived from the model of Figure 6 with appropriate scaling.

[17] Probably the small component of remanence in the direction of H_{TRM} is likewise a CRM, formed by alteration of TRM-carrying magnetite to hematite during demagnetization. Blocking temperatures up to slightly in excess of 525°C are expected for the TRM, and alteration taking place before unblocking may produce hematite carrying an inherited remanence of TRM direction. The H_{TRM} component remaining after demagnetization to 600°C is proportional to the same part of initial remanence as the H_{CRM} component (Figure 7) and the continuing susceptibility decrease resulting from demagnetization heatings to temperatures in excess of 525°C indicates that further alteration did indeed take place during the demagnetization.

[18] In conclusion, it seems that the remanence after demagnetization to 600°C is mainly of CRM origin, but it is not possible to assess whether it is the sum of individual components with the direction of NRM and H_{CRM}, respectively and similar blocking spectra, or if it is truly one component of intermediate direction formed in a resultant field as given by equation (1). The interpretation of the stable end components is not important for the practical implications for fold tests to be discussed in the remaining part of the paper.

6. Implications for Fold Tests

[19] The discussion will take two approaches: First, the data set will be treated as one case of alteration CRM formed in a fold and Second, the empirical relationship between v and u that appears to describe the CRM will be employed to explore more generally the consequences of CRM for fold tests in other fold configurations.

6.1. Unfolding the Experimental Data

[20] Stepwise unfolding of the CRM in the synthetic fold is shown in stereograms in Figure 9. The fold of the experiment is exceptional with its 130° folding angle exposing

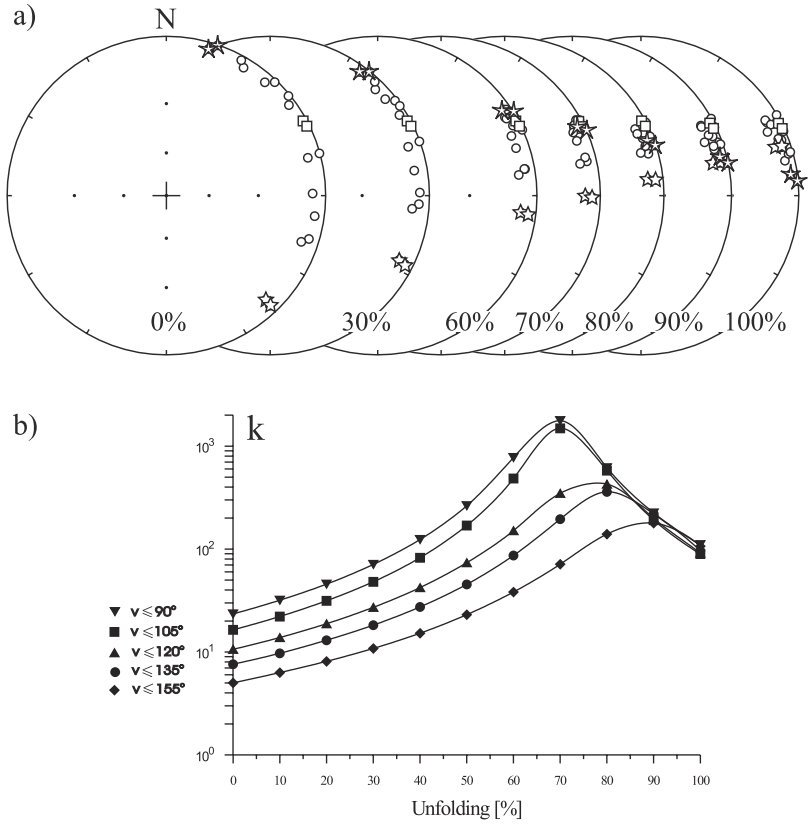

Figure 9. (a) Unfolding of the experimental CRM displayed in stereographic projection, with the fold axis vertical. Before unfolding "north" corresponds to the common direction of H_{CRM} and after full unfolding initial NRM directions are toward "east" for all specimens. Open symbols denote negative inclinations. The squares mark the data points from the middle specimens in the fold (Figure 2), which are stationary during unfolding. Data from the specimens at the ends of the fold are marked with two types of stars. (b) Improvement in alignment as indicated by the change of Fisher precision estimate k during unfolding. The lower curve (diamonds) shows the result obtained by unfolding the remanence of all specimens. The other curves are obtained by leaving out all specimens with v above the indicated value.

NRM to H_{CRM} at angles ranging from 25° to 155°, and it is therefore of equal interest to consider restricted parts of the fold. The part of the fold with CRM directions least consistent with a synfold magnetization is the part which had the higher angles to the remagnetizing field. As data points corresponding to highest v are removed two by two, k_{max} increases and the degree of unfolding for which k_{max} is obtained decreases from 90% toward 70% (Figure 9). At 70% all data points from v up to 105° coincide very well and removing more data does not give much further change in the statistics.

[21] To understand the fold test results of the synthetic fold it is instructive to consider the simpler case of CRM formation in only two blocks of different orientation to H_{CRM} (Figure 10). This situation is also of practical relevance, since in nature it is not always possible to find blocks of more than two different orientations. Both H_{CRM} and parent phase NRM are assumed to be perpendicular to the fold axis as in the experiment. In this case CRM of the two blocks will be accurately aligned for some degree of unfolding which may easily be derived:

[22] In accordance with the previous use of v and u, let v_1 and v_2 denote the angle from NRM to H_{CRM} for each of the two blocks and let u_1 and u_2 be the deflections of CRM from the NRM. The angle between remanence directions of the two blocks depends only on the relative unfolding, not on the final orientation of the unfolded stratum. To make the expressions simple, unfolding is performed by rotating each block the angle v in total. After $r \cdot 100\%$ unfolding the

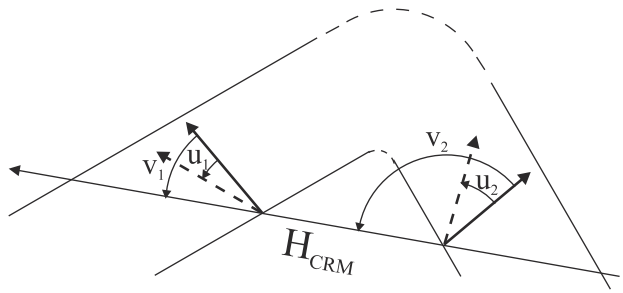

Figure 10. Post-tectonic CRM formation in two blocks of different tectonic correction, e.g., the limbs of a fold. CRM (dashed arrow) in both blocks formed in a direction intermediate between that of the parent phase NRM (full arrow), and the remagnetizing field, H_{CRM}.

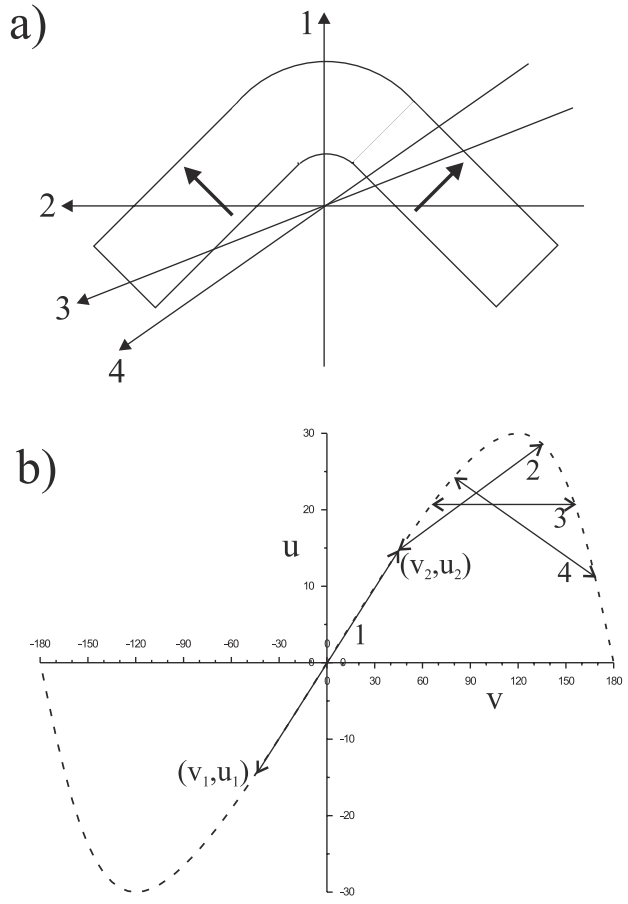

Figure 11. (a) Sketch of a fold with preexisting NRM indicated with bold arrows on the limbs. Arrows numbered 1–4 indicate different orientations of the remagnetizing field, H_{CRM}. (b) The curve from Figure 5 extended to the interval $[-180°; 180°]$. For each orientation of H_{CRM} shown in Figure 11a the points (v, u) corresponding to the two limbs are connected by a line, the slope of which determines the qualitative result of a fold test performed on the CRM of the two blocks.

blocks have been rotated the angle $r \cdot v$. The angle of CRM relative to H_{CRM} before unfolding is $v - u$ and after $r \cdot 100\%$ unfolding it is $v - u - rv$ or $(1 - r)v - u$. Requiring this angle to be the same for the two blocks, yields

$$(1 - r)v_1 - u_1 = (1 - r)v_2 - u_2, \tag{2}$$

from which r, the ratio of unfolding required to align CRM, can be expressed as a function of u and v for the two blocks:

$$r = 1 - \frac{u_2 - u_1}{v_2 - v_1}. \tag{3}$$

From equation (3) and the curve of Figure 5 the qualitative fold test result is easily inferred for folds of various folding angle and different orientations of H_{CRM}. Knowing v_1 and v_2, the degree of unfolding required to align CRM of the two blocks is 1 minus the slope of a line drawn from (v_1, u_1) to (v_2, u_2) (Figure 11). For angles up to about 90°, v increases nearly proportionally with u, i.e., the slope $u/v = \alpha$ is constant and the best unfolding will be $(1\text{-}\alpha) \cdot 100\%$ independent of u and v. This is the reason why CRM for v up to 105° in the synthetic fold group almost perfectly at 70% unfolding (Figure 9). From scenarios 1 to 4 of Figure 11 the slope is decreasing. In scenario 3 it has reached zero and the angle of CRM deflection is identical in the two blocks, $u_1 = u_2$, indicating a pretectonic magnetization. With the negative slope, scenario 4 is a case where the best grouping of data will appear for more than 100% unfolding.

[23] For the synthetic fold consisting in essence of nine blocks of different orientations, the best grouping of CRM directions will be a compromise between CRM formed at low v which will all align very well at 70% unfolding, and CRM of the blocks corresponding to high v, which will drag the occurrence of best grouping toward a higher degree of unfolding while k_{max} decreases (Figure 9).

6.2. Statistic Evaluation of Erroneous Fold Tests

[24] From the above analysis it is clear that when introducing data from additional "blocks" in the hinge zone of a fold (Figure 11), the site means of all blocks will coincide at the same degree of unfolding when $|v|$ is less than about 90° for all blocks (case 1). In cases 2, 3 and 4 the optimum unfolding is not common to all pairs of blocks (different slopes for different pairs) giving rise to a less tight clustering for best unfolding.

[25] Until this point the discussion has focused on the special case where both the parent phase NRM and H_{CRM} are approximately perpendicular to the fold axis. When one or both are not, other situations arise where no unfolding will bring data clusters from different limbs perfectly together. If for instance the NRM has a substantial component parallel to the fold axis, the remanence vectors will trace out a small circle when folded (Figure 12). Subsequent CRM formation will in general place the remanence directions of different blocks on separate small circles relative to the folding axis, so that the magnetic vectors can no longer be brought to coincide by unfolding.

[26] The above examples demonstrate that for some geometries reduced overlap of individual site means leaves a chance to detect by suitable fold test statistics that the fold test is in error. Other effects like undetected tectonic rotations, strain or failure to isolate individual components properly may affect the fold test in the same way as CRM, and it is important to find appropriate statistic methods to reject such erroneous fold tests. A number of statistical criteria have been proposed to judge the significance of fold tests and they are not equally well suited to deal with the problems put forward here.

[27] The classic test of *McElhinny* [1964], testing whether unfolding leads to a significant improvement in k, is not suited to reveal errors due to CRM or other undetected complications. Although the test is shown to be statistically invalid [*McFadden and Jones*, 1981] it is still widely used, often justified by noting that it is typically conservative compared to a valid test. This is probably true in cases where the original distribution is indeed restored for some degree of tectonic correction. The McElhinny test then requires a more severe folding than a valid test, in order to provide a significant improvement in k [*McFadden and Jones*, 1981]. However, when the best overlap of site means is reduced due to some undetected event, then as long as the

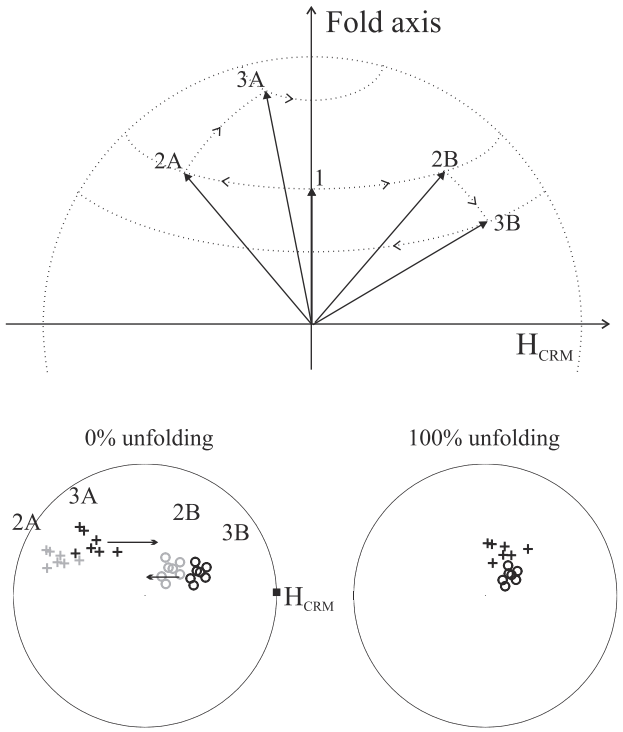

Figure 12. CRM formation in a fold when NRM has a component along the fold axis. (1) NRM of two blocks, A and B, before folding. (2) NRM after folding. At this stage the remanence directions (2A and 2B) of the two blocks can be reassembled by unfolding. (3) CRM with direction intermediate between H_{CRM} and NRM of each block. CRM directions (3A and 3B) of the two blocks will be on separate small circles when unfolding and can not be made to coincide by any degree of unfolding. Viewed in stereographic projection, CRM of the two blocks (solid crosses and circles) will follow separate tracks when unfolding, the site means passing by each other with poor overlap. Grey points indicate the NRM directions before chemical alteration.

folding is sufficiently severe, the McElhinny test will accept cases which may be rejected by a valid test. Hence the McElhinny test is not as safe to use as commonly thought. The CRM case of Figure 12 is one example where the grouping for best unfolding is obviously suspicious but nonetheless is significantly better than for the unfolded data according to the McElhinny test.

[28] The class of tests turning the fold test into a parameter estimation problem [*Watson and Enkin*, 1993; *Tauxe and Watson*, 1994]. are also not suitable to deal with undetected complications. These tests employ monte carlo techniques to determine, with an interval of confidence, the degree of unfolding resulting in the tightest cluster of site means. It is an implicit assumption that the occurrence of best grouping will indicate the timing of remanence acquisition relative to folding. *Tauxe and Watson* [1994] themselves showed that this basic assumption may fail in the case of undetected tectonic rotation, and the same applies to the case of CRM addressed here. Since there is no procedure included to assess how well individual site means are brought together, errors in the data caused by, e.g., CRM are unlikely to be detected.

[29] The fold test of *McFadden and Jones* [1981] has a potential of detecting errors revealing themselves in poor overlap of site means for all degrees of unfolding. It is tested whether, after a given tectonic correction, it is likely that the magnetic directions from different blocks were drawn from the same Fisher distribution. Qualitatively, this seems not to be the case with data like those of Figure 12 and the hypothesis of prefolding or synfolding magnetization may be rejected.

[30] Another approach by *McFadden* [1990] is to test for a correlation between the tectonic corrections and the distribution of site-mean directions about the overall mean direction. Taking again Figure 12 as an example, such a correlation clearly exists in that data points from the two limbs (i.e., subject to different tectonic corrections) cluster at separate sides of the restored mean direction. The test has gained limited attention, but the idea seems to work in this respect.

[31] The data set from the experiment, with nine "limbs" each represented by only two specimens, does not lend itself to fold test statistics. In section 6.3 the performance of fold tests, mainly the *McFadden* [1990] test, will be investigated using synthetic data simulated for various cases of intermediate direction CRM in folds.

6.3. Simulating CRM In a Fold

[32] Synthetic data were generated from a simple model utilizing the relationship between v and u indicated by the curve in Figure 5. Pretectonic NRM directions for each block were drawn from a Fisher distribution [*Fisher*, 1953] and rotated according to the position in the fold. CRM was simulated by adding to each NRM unit vector a vector of length 0.5 in the direction of H_{CRM}. Finally, conventional stepwise unfolding was applied to the resulting CRM directions.

[33] *McFadden and Jones* [1981] stress that before performing the fold test it should be demonstrated that the scatter of remanence directions in different parts of the fold are in agreement with the hypothesis that they are drawn from a common original population. The hypothesis of a common Fisher precision κ will frequently be rejected for data derived from the model described above due to the effect illustrated in Figure 13. When H_{CRM} is applied at low angles to a group of NRM directions, the addition of a component parallel to the field will contract the distribution, while at high angles it will expand it. However, simulations demonstrated that f is not very sensitive to precision variations of the magnitude in question. In the following

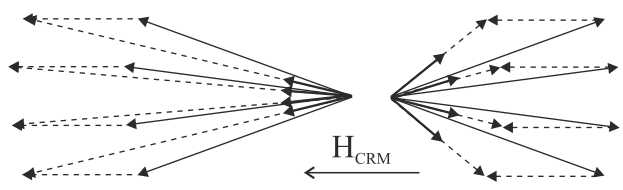

Figure 13. CRM modeled by adding the same vector (parallel to H_{CRM}) to a group of Fisher distributed NRM, will have reduced scatter relative to the NRM distribution when H_{CRM} is applied at low angles to NRM and increased scatter when it is applied at high angles. Full arrows: NRM, dashed arrows: "CRM formation" and bold arrows: resulting CRM directions.

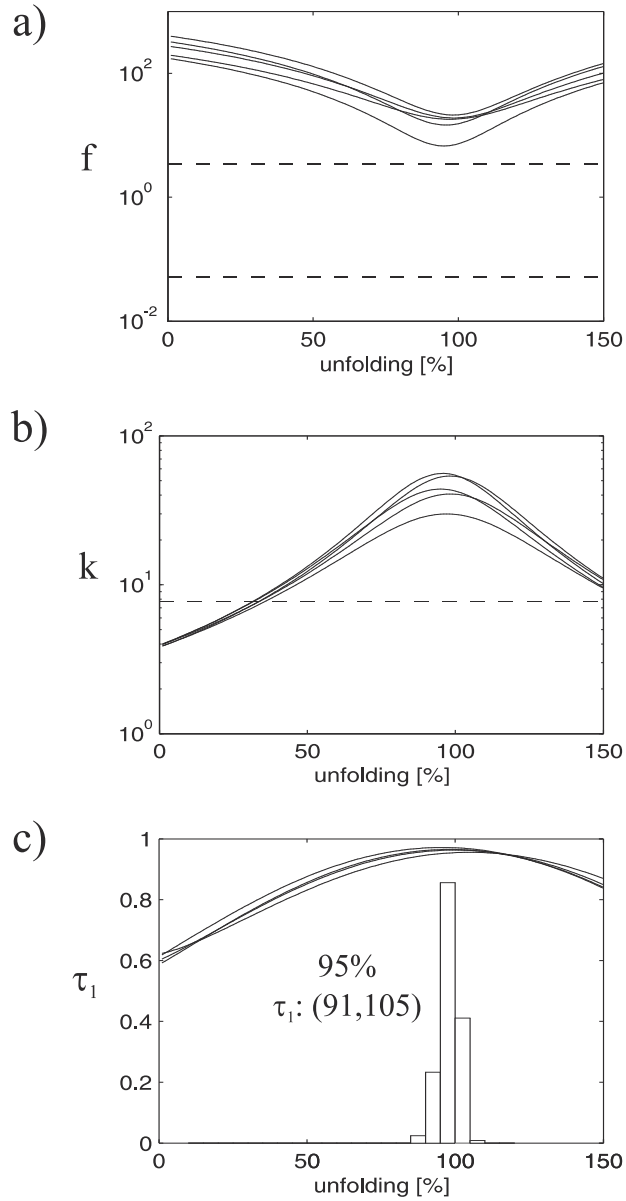

Figure 14. Statistic evaluation of synthetic data corresponding to scenario 3 of Figure 11 with original NRM inclined 20° from the vertical in the direction of the fold axis. For each limb 7 (13 for the bootstrap method (Figure 14c) data points were generated belonging to a Fisher distribution of $\kappa = 100$. The stereogram of Figure 12 displays one such data set. a) The f parameter of *McFadden and Jones* [1981] is not sufficiently close to unity (between dashed lines) to support a common origin of the remanence on different limbs at the 95% confidence level. (b) According to the criterion of the classic *McElhinny* [1964] test, k increases significantly after tectonic correction. Dashed line indicates the approximate level (slightly different for each data set) to be exceeded for significant improvement at the 95% confidence level. (c) The eigenvalue approach of *Tauxe and Watson* [1994]. High τ_1 (and low τ_2 and τ_3, not shown) indicates best grouping around 100% unfolding. The histogram displays the distribution of maximum τ_1 occurrence from 500 simple bootstrap pseudo data sets. The 95% confidence interval indicated includes 100% unfolding.

examples the McFadden and Jones fold test has been carried out ignoring that the criterion of a common precision was not always fulfilled.

6.4. Performance of Fold Test Statistics on Synthetic Data

[34] From a practical point of view it is often a more fatal error to falsely conclude a magnetization to be primary than mistaking it to be syntectonic, hence geometries close to that of scenario 3 (Figure 11) are of special interest and have been chosen to illustrate the points made about different types of fold test statistics. The stereograms of Figure 12 display one example of synthetic data, generated for a case like scenario 3, except that NRM has a component parallel to the fold axis (prefolding inclination −70°, declination coinciding with the horizontal fold axis). For similar data sets Figure 14 displays the fold test statistics of *McFadden and Jones* [1981], *McElhinny* [1964], and *Tauxe and Watson* [1994]. As expected from the qualitative assessment, the McFadden and Jones test successfully rejects the hypothesis of a common origin of the magnetization of the two limbs, while the McElhinny test and the parameter estimation technique indicates a common pretectonic origin of the magnetization.

[35] Figure 15 shows how components of NRM or H_{CRM} parallel to the fold axis affect the occurrence of best clustering in scenarios 1–4. When H_{CRM} is given a component parallel to the fold axis, the occurrence of best clustering in scenarios 1 and 2 is appreciably displaced toward 100%, increasing the chance of misinterpreting the magnetization to be pretectonic.

[36] Including more blocks in the analysis is not always an advantage. When NRM or H_{CRM} is not perpendicular to the fold axis, additional data from blocks of intermediate dips will tend to fill the gap between the data clusters of the limbs (Figure 12) and make the clustering appear better. However, when NRM and H_{CRM} are both perpendicular to the fold axis there is no chance to detect the presence of CRM if data are not available from more than two blocks. In this case the success of the McFadden and Jones test in correctly rejecting the hypothesis of prefolding or synfolding magnetization improves from scenarios 1 to 4 (Figure 11) as demonstrated by a few simulations (Figure 16). In scenario 1, as expected, the CRM is almost always accepted as a synfold magnetization. In scenario 4, a common origin of remanence is rejected in most cases.

6.5. Syntectonic CRM

[37] In the modeled cases (Figures 14, 15, and 16) the McFadden test owes its success to some extent to the quite large folding angle of the fold in the example (Figure 11). With smaller folding angles it will be more difficult to detect the CRM. This is worth noting when considering syntectonic CRM, since the folding angle at the time of remagnetization will be less severe than that of the final fold. If CRM forms in a short time compared to the period of the folding, the behavior of syntectonic CRM in fold tests may be derived from the previous discussion. Apart from smaller folding angles the difference will be the additional folding after CRM has formed. Unfolding will first bring back CRM directions as they were when formed in the partly folded rock. This situation is equivalent to the case of

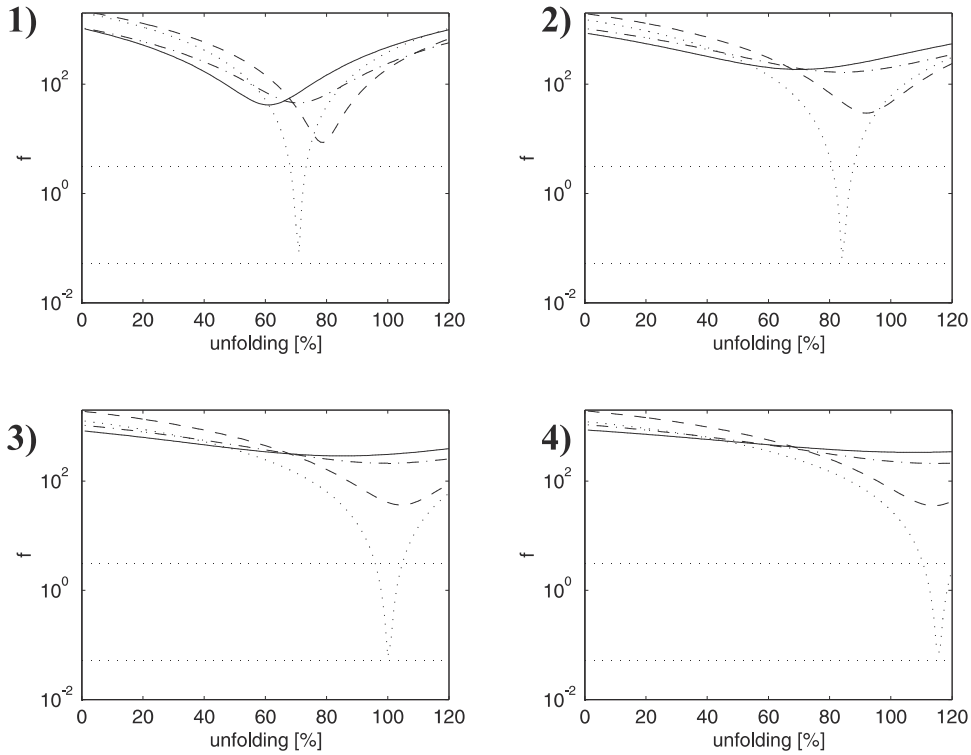

Figure 15. Synthetic data corresponding to scenarios 1–4 of Figure 11 with data from the limbs only. Dotted line, NRM and H_{CRM} perpendicular to the fold axis, shown for reference. Solid, dashed, and dash-dotted line, NRM, H_{CRM}, and both having a component parallel to the fold axis of size equal to the perpendicular component, respectively. For each limb, 25 data points were generated belonging to a Fisher distribution of $\kappa = 150$. Because of excellent data and relatively large remanence component parallel to the fold axis, the McFadden and Jones test in all cases rejects a common origin of magnetization.

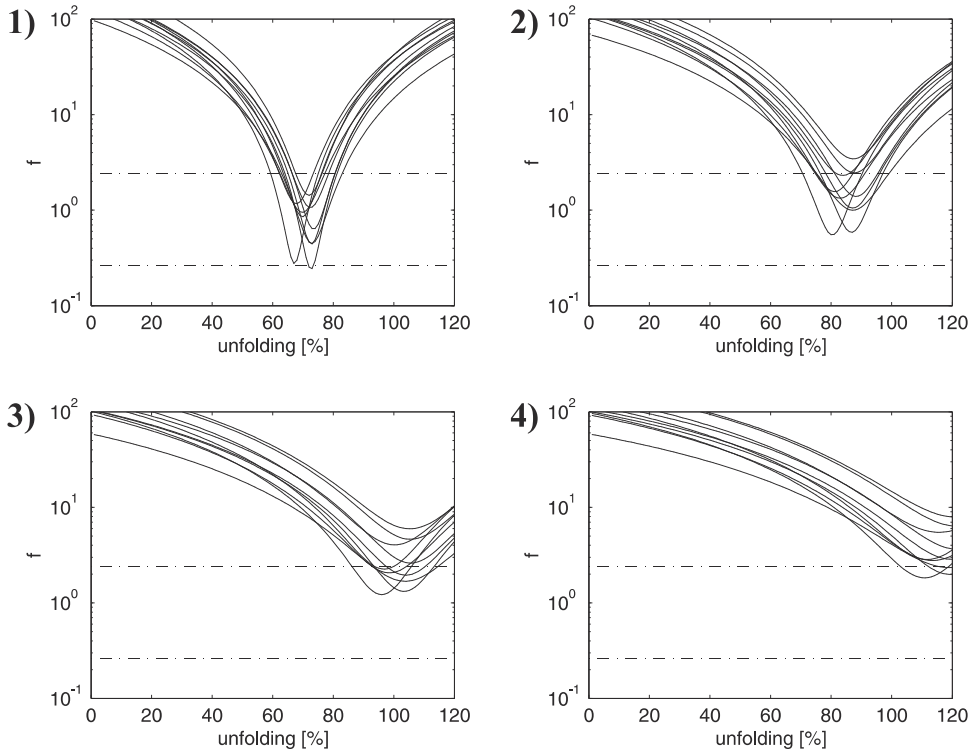

Figure 16. Synthetic data corresponding to scenarios 1–4 of Figure 11, assuming two blocks in the hinge zone in addition to the limbs. The dip of the hinge zone blocks were taken to be half the dip of the limbs, and for each block, 5 data points were generated belonging to a Fisher distribution of $\kappa = 150$.

post tectonic CRM studied so far and the insights from this study will apply to the remaining unfolding. However, the degree of unfolding for which the best grouping is obtained will be squeezed toward 100%, since unfolding from the point of CRM formation no longer corresponds to full unfolding from 0 to 100%, but only to the last part of it. Consider for instance scenario 1 of Figure 11. If CRM formed at 50% folding, the best grouping which would have occurred at around 70% unfolding had the CRM been post-tectonic, now occurs at around 85% unfolding. This will increase the chance of misinterpreting the magnetization to be pretectonic. Since tectonism is typically associated with heating and an environment facilitating chemical changes, syntectonic CRM is very common.

6.6. Intensity Variations Due to CRM

[38] The above analysis has demonstrated that for some geometries the chances are good that sensible fold test statistics will detect problems with data due to CRM, for other geometries it will be practically impossible. In addition to evaluating the fold test, a careful analysis of the intensity of remanence may help identify CRM in a fold. According to the results of Figure 8 the intensity varies by a factor of 3 when the angle of application of H_{CRM} change from parallel to antiparallel relative to the parent phase NRM. Hence if the intensity of remanence is observed to vary in a systematic way over the fold, and the variation can not be ascribed to variable mineralogy, this may indicate the presence of intermediate direction CRM. In the case of two blocks, a systematic variation is simply that the intensity in one block is significantly higher than in the other. As illustrated by Figure 13, high (low) intensities may be expected to be associated with high (low) k. Unfortunately, these variations are least for geometries like scenario 1 and for (syntectonic) CRM in folds of small folding angle, the same cases for which the fold test is least successful.

7. Conclusions

[39] From the experimental results and study of synthetic data, the following conclusions can be drawn concerning alteration CRM of intermediate direction and its effect on fold tests:

1. Oxidation of a low-Ti TM phase in basaltic specimens resulted in stable end-components with directions intermediate between H_{CRM} and the parent phase NRM. Both direction and strength of the end-components are well described by CRM formation in a resultant field obtained by vectorial addition of field components along NRM and H_{CRM}, or equivalently by vectorial addition of individual remanence components in these directions.

2. Stepwise unfolding of CRM in the ''fold'' of the experiment yields a syntectonic fold test result at statistical confidence level exceeding 95% using the McElhinny criteria. Considering other geometries it appears that pretectonic fold test results may also be obtained as artifacts of alteration CRM.

3. There are geometries for which no fold test will be able to distinguish post-tectonic CRM from a syntectonic or pretectonic magnetization, even with high-quality data. In other cases it may be possible, for instance when H_{CRM}, or especially parent phase NRM has a substantial component parallel to the fold axis. If remanences are approximately perpendicular to the fold axis it is crucial to have data from more than two blocks of different orientation.

4. Not all proposed fold test statistics are suited to deal with the problems put forward here. In many cases the McFadden and Jones test applied to synthetic CRM data, correctly rejected the hypothesis of prefold or synfold magnetization. The McElhinny test and the parameter estimation approach proved inappropriate to reveal the effects of CRM. In particular, this exemplifies that use of the McElhinny test can not be justified with reference to its conservatism as commonly stated. Other conditions like undetected tectonism and strain probably can affect fold tests in a way similar to that of CRM. Hence statistics for evaluating fold tests should be selected with caution.

5. A systematic variation of intensity and/or the precision of data over a fold may indicate the presence of CRM.

[40] **Acknowledgments.** Reidar Løvlie is thanked for measuring hysteresis properties of the rock. We also thank Mike Jackson for constructive comments to the interpretation of the experiment and two anonymous reviewers who helped clarify the manuscript. The first author is in receipt of a Ph.D scholarship from the Danish Research Council.

References

Bailey, M. E., and C. J. Hale, Anomalous magnetic directions recorded by laboratory-induced chemical remanent magnetization, *Nature*, *298*, 739–741, 1981.

Fisher, Dispersion on a sphere, *Proc. R. Soc. London, Ser. A*, *217*, 295–305, 1953.

Heider, F., and D. J. Dunlop, Two types of chemical remanent magnetization during the oxidation of magnetite, *Phys. Earth Planet. Inter.*, *46*, 24–45, 1987.

Lowrie, W., Identification of ferromagnetic minerals in a rock by coercivity and unblocking temperature properties, *Geophys. Res. Lett.*, *17*, 159–162, 1990.

McElhinny, M. W., Statistical significance of the fold test in paleomagnetism, *Geophys. J. R. Astron. Soc.*, *8*, 338–340, 1964.

McFadden, P., A new fold test for paleomagnetic studies, *Geophys. J. Int.*, *103*, 163–169, 1990.

McFadden, P. L., and D. L. Jones, The fold test in paleomagnetism, *Geophys. J. R. Astron. Soc.*, *67*, 53–58, 1981.

Pullaiah, G., E. Irving, K. L. Buchan, and D. J. Dunlop, Magnetization changes caused by burial and uplift, *Earth Planet. Sci. Lett.*, *28*, 133–143, 1975.

Tauxe, L., and G. S. Watson, The fold test: An eigen analysis approach, *Earth Planet. Sci. Lett.*, *122*, 331–341, 1994.

Walderhaug, H., Directional properties of alteration CRM in basic igneous rocks, *Geophys. J. Int.*, *111*, 335–347, 1992.

Walderhaug, H. J., T. H. Torsvik, and R. Løvlie, Experimental CRM production in a basaltic rock; evidence for stable, intermediate directions, *Geophys. J. Int.*, *105*, 747–756, 1991.

Walton, D., Time-temperature relations in the magnetization of assemblies of single-domain grains, *Nature*, *286*, 245–247, 1980.

Watson, G. S., and R. J. Enkin, The fold test as a parameter estimation problem, *Geophys. Res. Lett.*, *20*, 2135–3137, 1993.

K. N. Madsen and H. Walderhaug, University of Bergman, Institute of Solid Earth Physics, Allégaten 41, N-5007 Bergman, Norway. (karen.madsen@ifjf.uib.no)

T. Torsvik, VISTA, c/o Geological Survey of Norway, PB 3006 Lade, N-7002 Trondheim, Norway.